Advanced Composite Materials
Publication details, including instructions for authors and subscription information:
http://www.tandfonline.com/loi/tacm20

Effect of rotational imbalance on fracture rotation speed of carbon-carbon ring

Ken Goto , Hiroshi Hatta , Yuichi Nishiyama , Taro Higuchi & Toshio Sugibayashi

Version of record first published: 02 Apr 2012.

To cite this article: Ken Goto , Hiroshi Hatta , Yuichi Nishiyama , Taro Higuchi & Toshio Sugibayashi (2004): Effect of rotational imbalance on fracture rotation speed of carbon-carbon ring, Advanced Composite Materials, 13:3-4, 283-296

To link to this article: http://dx.doi.org/10.1163/1568551042580217

Adv. Composite Mater., Vol. 13, No. 3-4, pp. 283–296 (2004)

Also available online - www.vsppub.com

Effect of rotational imbalance on fracture rotation speed of carbon-carbon ring

KEN GOTO [1], HIROSHI HATTA [1,*], YUICHI NISHIYAMA [2], TARO HIGUCHI [3] and TOSHIO SUGIBAYASHI [4]

[1] *The Institute of Space and Astronautical Science, Japan Aerospace Exploration Agency, 3-1-1 Yoshinodai, Sagamihara, Kanagawa 229-8510, Japan*
[2] *Interdisciplinary Graduate School of Science and Engineering, Tokyo Institute of Technology, 4259 Nagatsuda-machi, Midori-ku, Yokohama, Kanagawa 226-8503, Japan*
[3] *Graduate School, Department of Material Science and Technology, Tokyo University of Science, 2641 Yamazaki, Noda, Chiba 278-8510, Japan*
[4] *Department of Mechanical Engineering, Takushoku University, 815-1, Tate-machi, Hachioji, Tokyo 193-0985, Japan*

Received 7 June 2004; accepted 23 July 2004

Abstract—Spin burst tests of carbon-carbon (C/C) rings were carried out to confirm the fracture criterion under high speed rotation as a function of the inner/outer diameter ratio $\bar{R}$. The C/C rings were made of a quasi-isotropic lamination type and were confirmed by static tensile tests to have isotropic strength. The burst rotation speeds of the C/C rings were found to be much lower than those expected from stress distributions. A detailed inspection of stress distributions in the C/C rings revealed that a rotational imbalance inherent in C/Cs caused a high average hoop stress and stress concentration around the inner radius. These effects were shown to lower fracture rotation speeds.

Keywords: Carbon/carbon composites; spin burst; turbine disk.

1. INTRODUCTION

Carbon-Carbon Composites (C/Cs) are the only lightweight material that maintains high strength and toughness at over 2000 K in an inert atmosphere. Based on this fact, C/Cs have been considered as a candidate material for a high temperature operating turbine disk to enhance heat efficiency [1, 2]. Some attempts to manufacture a turbine disk made with high temperature resistant composite materials like C/Cs or SiC fiber-reinforced SiCs (SiC/SiCs) have been made in the last two decades [1–4]. Although some of them resulted in a nicely shaped turbine

*To whom correspondence should be addressed. E-mail: hatta@isas.jaxa.jp

disk, none of them could successfully describe the fracture mechanism and criterion under high speed rotation.

We previously reported on the fracture and deformation of a two-dimensional laminated C/C ring under high speed rotation in conjunction with a development study of a carbon-carbon composite turbine disk [5]. The study revealed that the stress distribution in a C/C ring with the inner/outer radius ratio $\bar{R} = 0.21$ was consistent with linear elastic stress analysis up to the total fracture of the rings. In addition, fracture behavior of the un-notched ring was described by the average hoop stress criterion, that is, that the fracture occurs when mean stress in the circumference direction, $\bar{\sigma}_\theta$, reaches the static tensile strength.

In contrast, rings made of brittle materials like cast iron or poly-crystalline graphite failed by the average hoop stress criterion when $\bar{R} > 0.5$. However, they failed at lower rotation speeds than those predicted at $\bar{R} \leqslant 0.5$ because of stress concentration around the inner radius [6, 7]. The fracture rotation speed of laminate type CFRP disks was reported to be described by the maximum hoop stress criterion or Hoffman's fracture rule [8–10]. Moreover, the fracture behavior of SiC fiber-reinforced SiC (SiC/SiC) rings demonstrated contradictory results [4]. Quasi-isotropic laminate SiC/SiC rings ($\bar{R} = 0.30$) were reported to fail under the average hoop stress criterion, while the maximum hoop stress criterion successfully predicted the fracture rotation speed of r-θ-z three-dimensional fiber-reinforced SiC/SiC rings ($\bar{R} = 0.20$) [4].

The stress–strain relation of C/Cs is linear up to the ultimate fracture under monotonic tension, and fracture behavior looks brittle. On the other hand, C/Cs were reported to possess large fracture toughness by a fracture resistance mechanism that operates in front of a notch root [11, 12]. The mechanism responsible for the fracture resistance of C/Cs was believed to be different from that of SiC/SiCs, which was achieved by stress redistribution generated by stiffness reduction due to matrix fractures around a notch tip, though the details of the toughening mechanism have not been well elucidated. Hence, C/C rings might show notch sensitivity with a small $\bar{R}$ as a result of stress concentration around the inner radius, and the limitations of the average hoop stress criterion are still unclear.

Another mechanism that might lower fracture rotation speeds of C/C rings is the additional load generated by rotational imbalance. Disks made of high temperature fiber-reinforced composites like C/Cs or SiC/SiCs possess intrinsic rotational imbalance due to the non-uniformity of density distribution. In addition to non-uniformity of density, the adjustment of rotational balance by shaving off a thin piece of a ring is difficult because the shaving of the surface to achieve rotational balance might damage the reinforcing fibers and degrade their strength. Therefore, rotational imbalance tends to remain in the rings made of high temperature composites. However, the effect of the lack of rotational balance on fracture behavior under high speed rotation has not been elucidated; no detailed study has yet been reported.

This study focused on the effect of rotational imbalance on the fracture behavior of C/C rings, using spin burst tests of the C/C rings with a thickness gradient. The applicability of the average hoop stress criterion was also examined using C/C rings with various values of $\bar{R}$.

2. EXPERIMENTAL PROCEDURE

2.1. Materials

The C/C used in this study was a quasi-isotropic laminate type C/C with a stacking sequence of $[0°/45°/90°/-45°]_{4s}$ manufactured via the pre-formed yarn method [14] by Across Corporation (Saitama Japan). The reinforcing fiber was a PAN based high modulus type carbon fiber (TORAYCA® M40, Toray Co. Ltd., Tokyo, Japan; number of filaments = 6000), and fine coke powders and bulk meso-phase pitch were used as precursors of the carbon matrix. The final heat treatment temperature was set to 2273 K. The nominal volume fraction of the fiber was 0.5, with a bulk density of 1700 kg/m^3. The C/C rings were cut and shaped from 300 × 300 mm plates (nominal thickness = 3.0 mm) by the conventional milling technique. To change $\bar{R}$, the inner radius r_i was varied from 30 ($\bar{R} = 0.21$) to 126 mm ($\bar{R} = 0.90$) with a constant outer radius, r_o = 140 mm (Fig. 1). To avoid fiber damage due to machining, the C/C rings were not processed in the through-the-thickness direction. Figure 2 shows the thickness distribution of the C/C rings measured in the vicinity of the outer radius. The fact that the thickness distribution coincided with a sinusoidal curve means that the C/C plate where the rings were cut had constant inclination in the through-the-thickness direction. Three C/C rings cut from the same production batch plate possessed nearly identical thickness inclination, with a maximum thickness difference from the average thickness, Δt, of 0.2 mm.

2.2. Mechanical tests

2.2.1. Tensile test. The basic mechanical properties of the C/C were obtained by static tensile tests. Figure 3 shows the shape and dimensions of the specimen. Tensile tests were conducted by a screw-driven testing machine (AUTOGRAPH®, AG-5000A, Shimadzu Crop, Kyoto, Japan) with a constant crosshead speed of 0.1 mm/min in ambient air. Strain measurements were conducted by four strain gages (effective gage area = 2 × 5 mm) adhered parallel and perpendicular to the loading direction on both sides of the specimens. Tensile tests at 22.5° to the fiber axis were also conducted to ensure the effect of the loading direction on the mechanical properties.

2.2.2. Rotation test. Cold spin tests were carried out in a vacuum chamber using a spin tester driven by an air turbine (Maximum test weight = 10 kg, Maruwa Electric Corp., Chiba, Japan). The rotational balance of an assembled rotor as

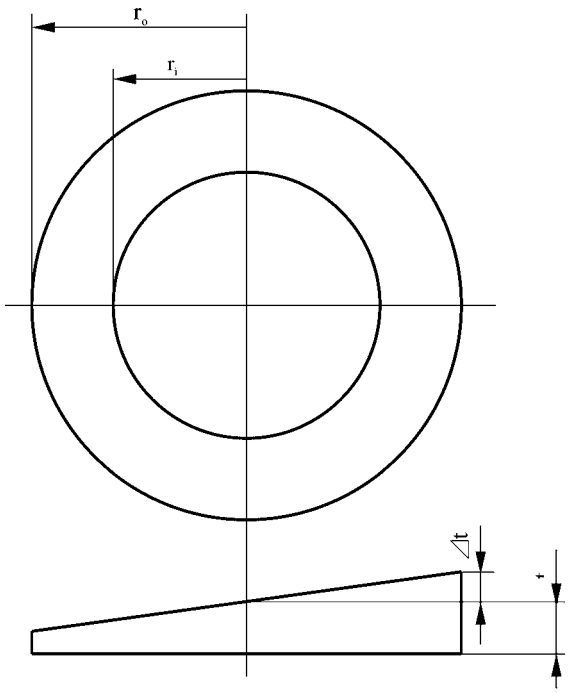

$\bar{R}$ (r_i/r_o)	0.21、0.5、0.7、0.9
r_o mm	70
t mm	3.2
$\cdot$ t mm	0.2

Figure 1. Shape and dimensions of the C/C rings used for spin burst tests.

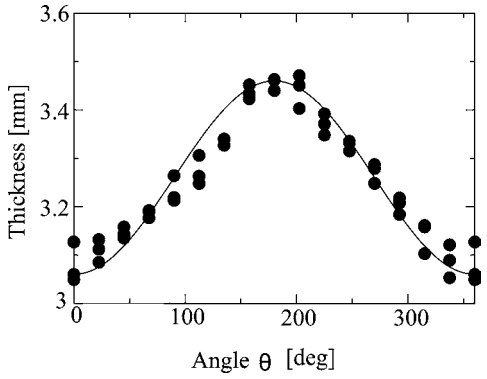

Figure 2. Typical distribution of thickness in the C/C ring.

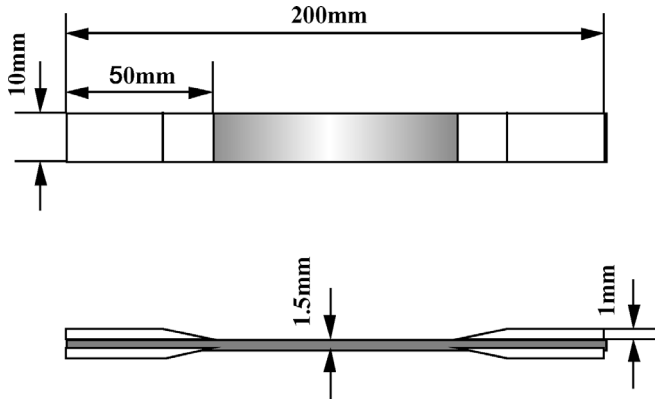

Figure 3. Shape and dimensions of tensile test specimen.

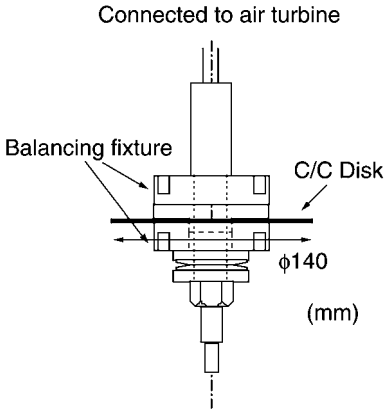

Figure 4. Rotation fixture assembled with the C/C ring.

shown in Fig. 4 was adjusted by a rotational balance tester (FH216, Akashi Co. Ltd., Kanagawa, Japan). To avoid fiber damage from additional shaving, the rotational balance of the C/C rings was not adjusted, but rather the weight of the fixture was adjusted to achieve smooth rotation. Rotation tests were conducted with a constant acceleration speed of 100 rpm/s at a reduced pressure of less than 10 Pa at room temperature. Figure 5 shows a schematic drawing of a setup of the spin tester. A fine copper wire (diameter = 0.5 mm) was set around the specimen to detect the fracture of a specimen by the fractured fragments cutting the wire. The fractured fragments of the C/C rings were captured inside a rubber tire stuffed with soft felt.

2.3. Finite element analysis

The stress distribution in the C/C rings was computed by finite element analysis (FEA) using the commercially available software ABAQUS version 5.8. Half of the symmetrical ring was modeled as shown in Fig. 6. The mesh was composed of eight node shell-type elements, and thickness was inclined from left to right with a

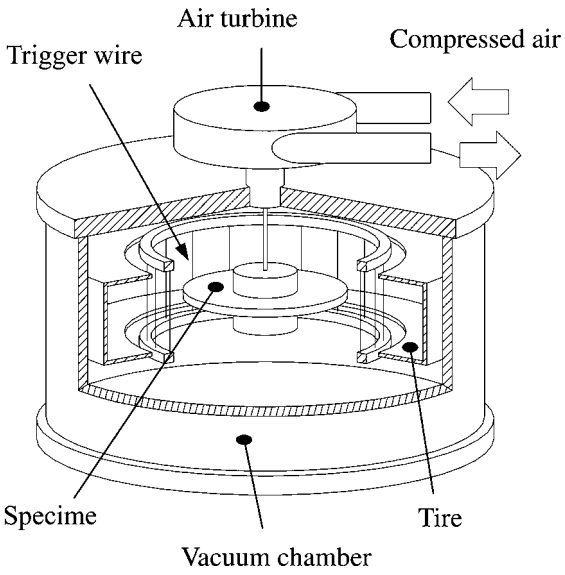

Figure 5. Schematic drawing of the spin burst tester.

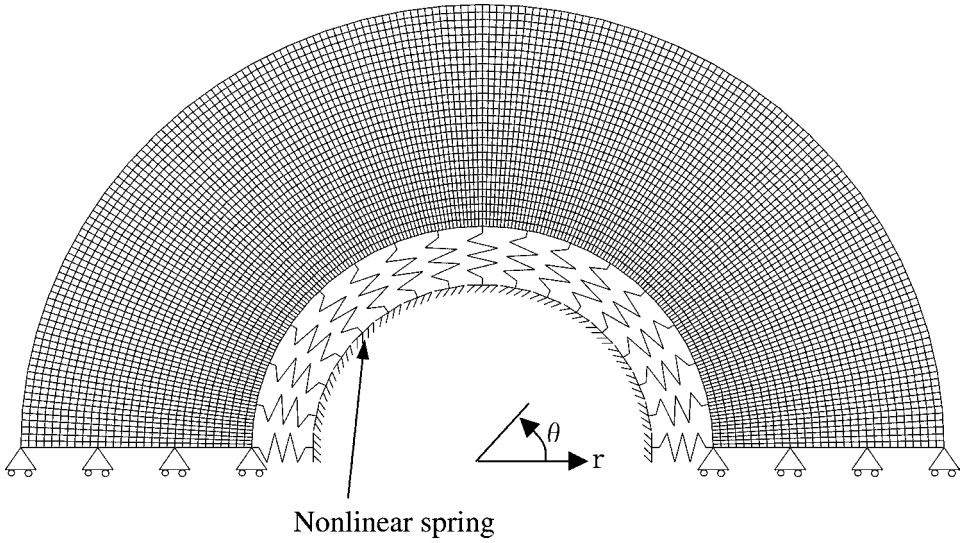

Figure 6. A FEM model used for determination of stress distributions in the C/C ring.

constant gradient as shown in Fig. 2. The constraint from the rotational fixture was simulated by non-linear spring elements that, by changing spring constants, deform freely under tension but not under compression. The effect of the non-linear spring elements on the analytical results was clarified by enlarging the spring constant in compression tenfold, and the computed results were not affected. Displacement of the nodes in the radial direction of the model at the inner radius was also confirmed not to be negative. The analysis was conducted under the assumption

of linear elastic response using isotropic mechanical properties, Young's modulus, $E = 56$ GPa, and Poisson's ratio, $\nu = 0.3$, obtained from tensile tests ($n = 3$). The centrifugal force $\rho\omega^2$, where ρ is density and ω is angular velocity, was applied to all the elements of the mesh with its rotational center at the center of the mesh.

3. RESULTS AND DISCUSSIONS

3.1. Tensile test

Basic tensile deformation and fracture behaviors of the C/C were examined by tensile tests in parallel and at 22.5° to the fiber axis. Stress–strain curves of both 0° and 22.5° samples were linear up to the total fracture with the same Young's modulus and the tensile strength. In addition, the shear mechanical properties of the C/C were also reported to be independent of the inclination angle [11]. Thus, the C/C in this study was proved to possess linear isotropic mechanical properties, Young's modulus, $E = 65$ GPa ($n = 3$), Poisson's ratio, $\nu = 0.3$ ($n = 3$), and the tensile strength, $\sigma_s = 165 \pm 10$ MPa ($n = 5$).

3.2. Spin burst test

C/C rings failed by σ_θ as shown in Fig. 7. $\bar{\sigma}_\theta$ of the C/C ring with uniform thickness and density distribution is given by [15],

$$\bar{\sigma}_\theta = \frac{1}{3}\rho\omega^2 r_o^2\left(\bar{R}^2 + \bar{R} + 1\right). \tag{1}$$

$\bar{\sigma}_\theta$ of the C/C rings estimated from equation (1) with various $\bar{R}$ at fracture rotation speed are shown in Fig. 8 as open circles. In Fig. 8, closed circles represent fracture rotation speed. Here, one of the C/C rings with $\bar{R} = 0.9$ failed at a lower rotation speed due to the enormous vibration of the rotor caused by some trouble with the spin tester. Hereafter, the result of this ring is distinguished by parentheses from other results, as shown in Fig. 8 and also Fig. 12. Figure 8 implies that the fracture occurred under the average hoop stress criterion at $\bar{R} \geqslant 0.6$. However, $\bar{\sigma}_\theta \approx 140$ MPa at fracture rotation speeds was clearly lower than the static tensile strength of the C/C (165 MPa).

3.3. Stress analysis

One of the reasons $\bar{\sigma}_\theta$ at fracture rotation speeds became lower than the static tensile strength is the stress enhancement caused by rotational imbalance resulting from non-uniformity of thickness. Stress distributions in the C/C rings with thickness gradient were computed by FEA with various values of $\bar{R}$. Figures 9a to 9c show the contour maps of σ_θ at fracture rotation speeds in the C/C ring ($\Delta t = 0.2$ mm) with $\bar{R} = 0.21$, 0.70, and 0.90, respectively. In Fig. 9, the right hand side is the area having the larger thickness. The effect of the thickness gradient on stress

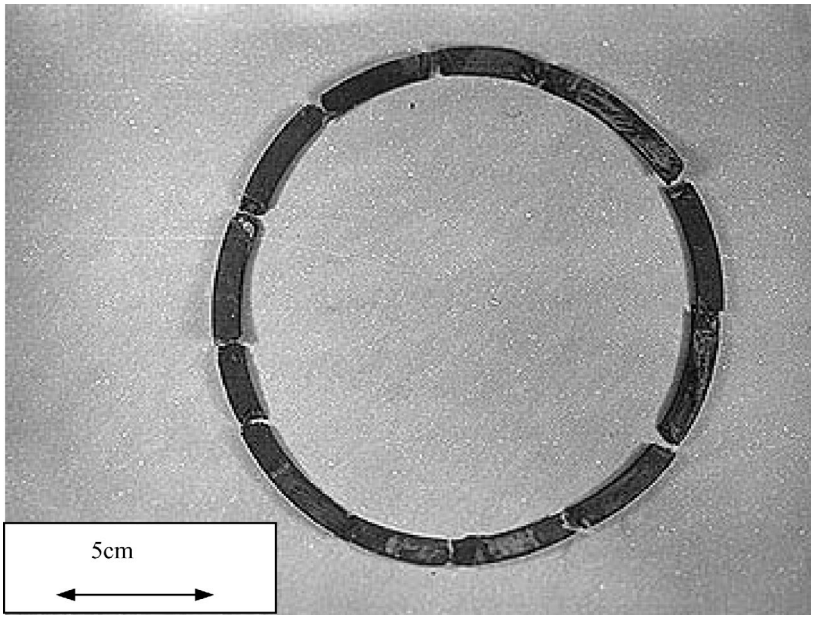

(a)

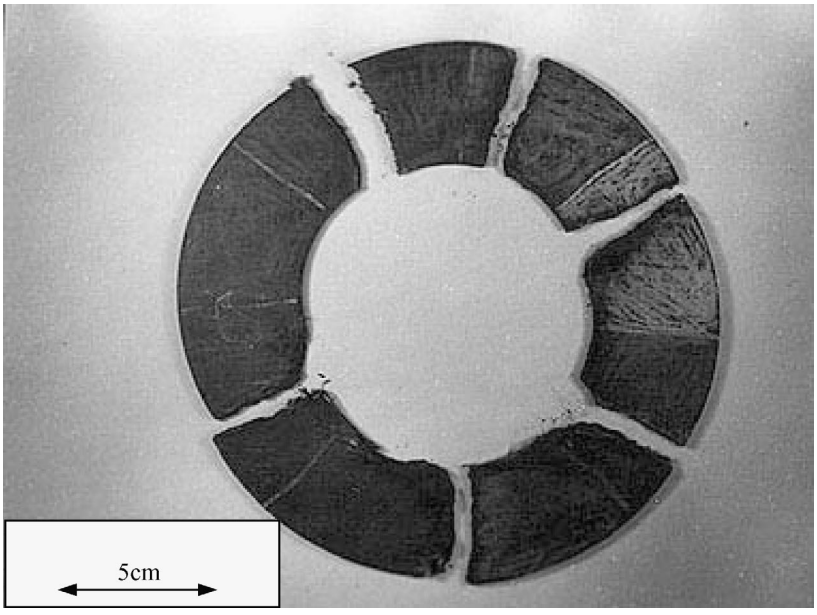

(b)

Figure 7. Fracture patterns of C/C rings. (a) $\bar{R} = 0.90$, (b) $\bar{R} = 0.70$.

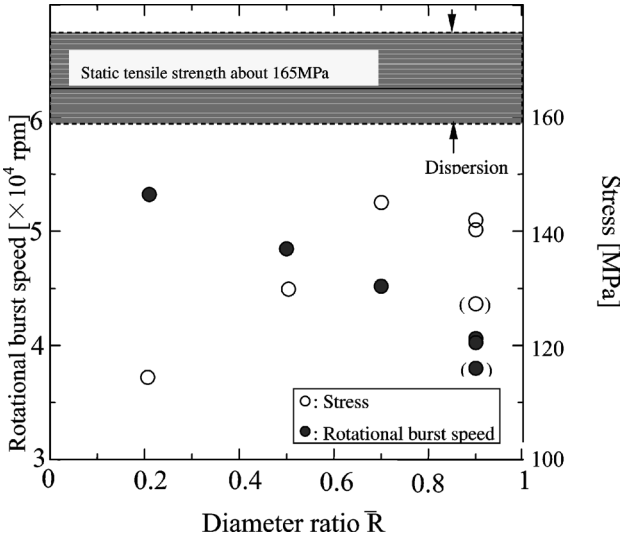

Figure 8. Spin burst speeds and circumferential mean stresses at the burst speeds as a function of radius ratio $\bar{R}$.

distributions can be observed as deviations of a stress contour map from the case of a ring with uniform thickness, which appears as a series of concentric circles. Thus, the deviations of stress distribution in the center area of the models in Fig. 9, where the thickness has average value, is generated by rotational imbalance caused by the thickness gradient. The deviation of stress distribution occurred due to additional bending caused by deformation of the ring into an elliptic shape by rotational imbalance, and σ_θ takes its maximum value ($\sigma_\theta^{\max}$) at the inner radius of the ring. The location of $\sigma_\theta^{\max}$ moved to the thicker area of the ring with the increase of $\bar{R}$. In addition, the maximum value of $\bar{\sigma}_\theta$, $(\bar{\sigma}_\theta)_{\max}$, showed the same tendency as $\sigma_\theta^{\max}$, although the location of $(\bar{\sigma}_\theta)_{\max}$ was slightly different from that of $\sigma_\theta^{\max}$. Figures 10a and 10b show $(\bar{\sigma}_\theta)_{\max}$ and $\sigma_\theta^{\max}$ as a function of Δt, where the vertical axes, $<\bar{\sigma}_\theta>$ and $<\sigma_\theta^{\max}>$, were normalized by the values of $\Delta t = 0$. It is obvious that rotational imbalance due to the thickness gradient enlarges $(\bar{\sigma}_\theta)_{\max}$ and $\sigma_\theta^{\max}$ by about 5–15%.

3.4. Fracture of the C/C rings

The fact that deviations of stress distributions due to rotational imbalance were observed in the average thickness area (Figs 9a–9c) implies that additional centrifugal force in the larger thickness area of the ring generates additional hoop stress (Fig. 11). For the first order estimation of the stress enhancement, let us consider the load balance in the ring at sections A-A and B-B in Fig. 11. First, additional centrifugal force is generated on the right side of the ring (thicker area) and is supported by the cross-sections A-A and B-B. A counter force is generated from the rotation fixture on the left side of the ring (thinner area). In fact, the bending deformation

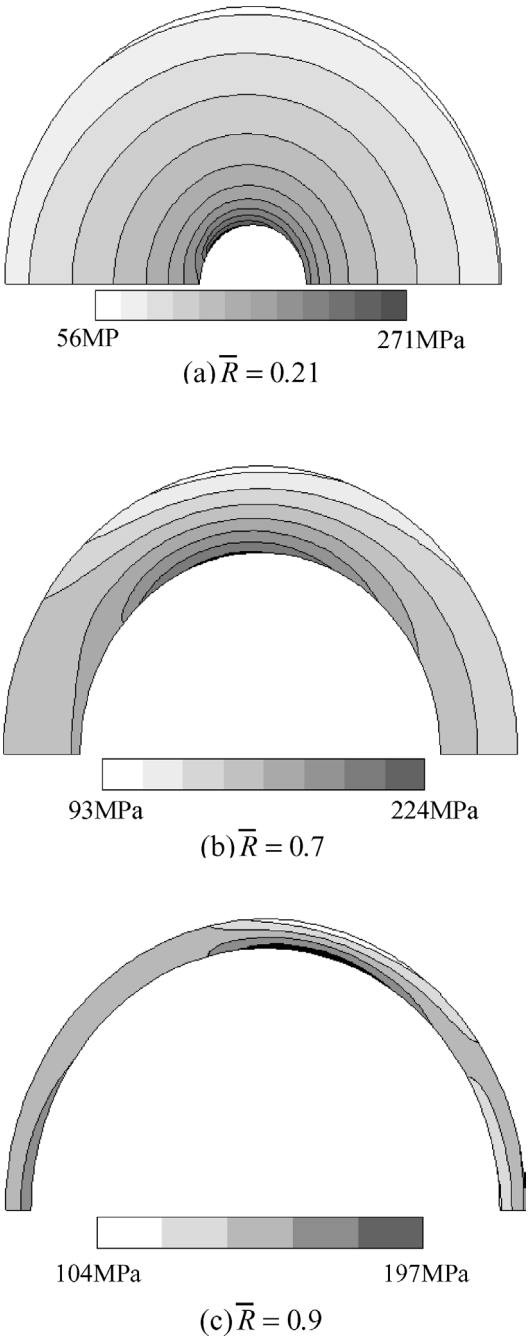

Figure 9. Distributions of circumferential normal stress σ_θ for rings with various inner/outer radius ratio $\bar{R}$ calculated from FEA.

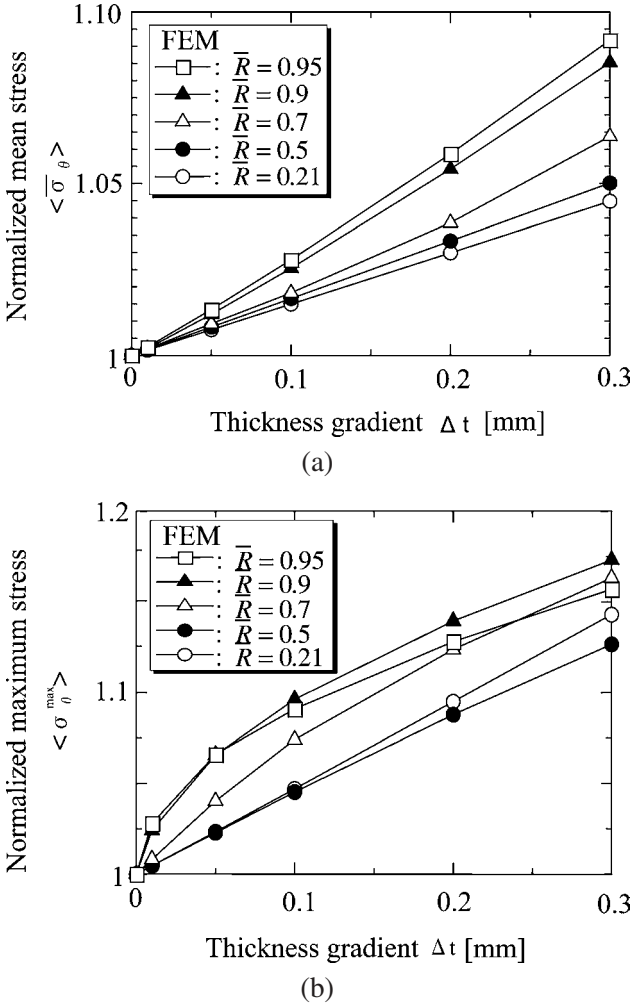

Figure 10. Normalized average circumferential stress $<\bar{\sigma}_\theta>$ (a) and maximum circumferential stress $<\sigma_\theta^{\max}>$ (b) as functions of thickness gradient Δt.

occurs in the vicinity of sections A-A and B-B. Its effect on the enhancement of hoop stress is slight, which allows the effect of the bending deformation to be ignored in the approximation. Additional centrifugal force by the thickness gradient can be expressed as

$$F = \frac{\pi\rho\omega^2\Delta t}{8r_\mathrm{o}}\left(r_\mathrm{o}^4 - r_\mathrm{i}^4\right), \tag{2}$$

when the thickness gradient, δt, is assumed to be uniform and given by

$$\delta t = \Delta t x/r_\mathrm{o} = \Delta t\,(r/r_\mathrm{o})\cos\theta. \tag{3}$$

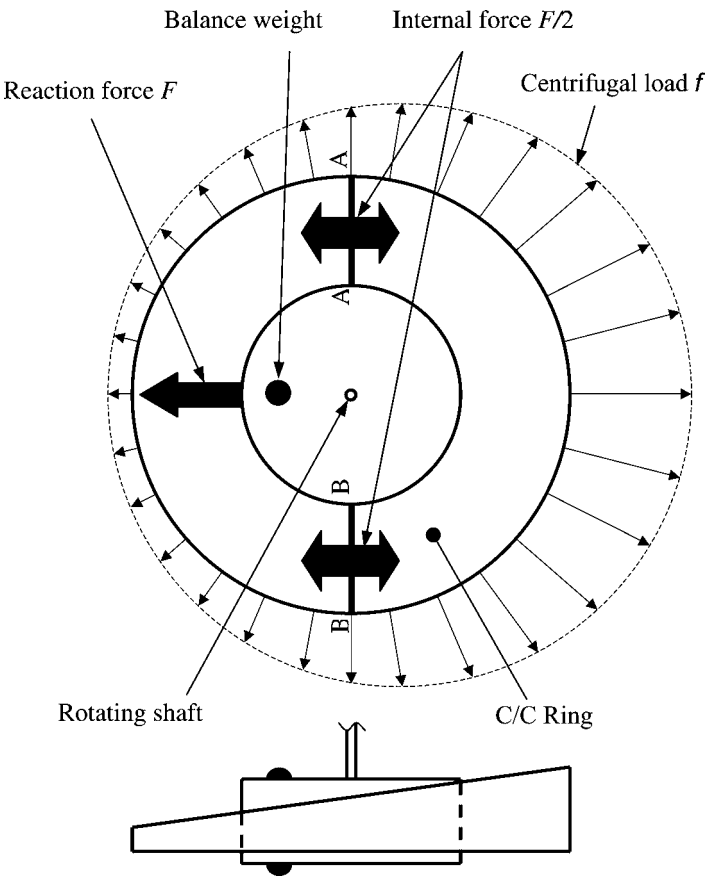

Figure 11. Schematic illustration of the effect of rotational imbalance on stress distribution in rotating rings.

Thus, the stress increment $\Delta\sigma_\theta$ in sections A-A and B-B is given by dividing F by the cross-sectional area, as

$$\Delta\sigma_\theta = \frac{\pi\,\Delta t}{16t}\rho\omega^2 r_o^2\left(\bar{R}^3 + \bar{R}^2 + \bar{R} + 1\right), \tag{4}$$

where t is the average thickness. $\bar{\sigma}_\theta$ from FEA agrees well with the predicted value from equation (4). This finding indicates that the approximation given by equation (4) is valid for the estimation of $\bar{\sigma}_\theta$ enhancement in the C/C ring by the thickness gradient.

To examine the fracture criterion of the C/C ring, $(\bar{\sigma}_\theta)_{\max}$ and $\sigma_\theta^{\max}$ at fracture rotation speeds obtained by FEA are shown in Fig. 12 as functions of $\bar{R}$. From the figure, it is obvious that $\sigma_\theta^{\max}$ is inappropriate for fracture criterion with all $\bar{R}$. In contrast, $(\bar{\sigma}_\theta)_{\max}$ with the correction of stress enhancement by rotational imbalance in $\bar{R} \geqslant 0.6$ agrees well with static tensile strength. However, fracture speeds at $\bar{R} < 0.6$ appear to be affected by stress concentration in the inner radius of the ring,

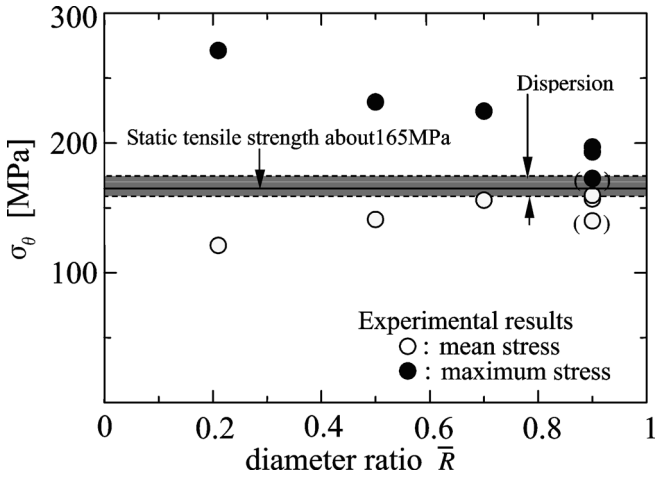

Figure 12. Comparison of maximum stress and average stress criteria.

given that $(\bar{\sigma}_\theta)_{\max}$ at fracture speed became lower than the static tensile strength. As described earlier, $\sigma_\theta^{\max}$ of the rings at $\bar{R} < 0.6$ is clearly larger than the static tensile strength. Therefore, $\sigma_\theta^{\max}$ cannot be applicable as the fracture criterion of the C/C rings in the region of $\bar{R} < 0.6$. This finding suggests that the fracture resistance mechanism of C/Cs that operates in front of a crack tip during crack extension also operates at the stress-concentrated area in the C/C ring at $\bar{R} < 0.6$.

4. CONCLUSIONS

Spin burst tests of quasi-isotropic laminate C/C rings were conducted to clarify fracture behaviors, and the following conclusions were obtained.

(1) Rotational imbalance by non-uniformity of the thickness or density enhanced the stresses generated in the C/C rings and apparently degraded the strength of the ring.

(2) The C/C rings failed under the average hoop stress criterion at $\bar{R} \geqslant 0.6$. Because of stress concentration around the inner radius, the spin burst speed decreased from the prediction of the average hoop stress criterion at $\bar{R} < 0.6$.

(3) Stress enhancement in the C/C ring due to rotation imbalance caused by the thickness gradient was successfully predicted by a simple approximation.

Acknowledgements

Part of this work was carried out with the support of a grant-in-aid for basic science (grant No. 11305047) from the Ministry of Education, Sports, Culture, Science, and Technology of Japan.

REFERENCES

1. D. L. Schmidt, K. E. Davidson and L. S. Theibert, *SAMPE J.* **35** (3), 27 (1999).
2. H. Hatta, Y. Kogo, N. Tanatsugu, H. Onabe, T. Mizutani, H. Kawada and S. Shigemura, *ISAS Report* **85**, 1–26 (1996).
3. J. W. Brockmeyer, *Trans. ASME, J. Engng. for Gas Turbines and Power* **115**, 58–63 (1993).
4. N. Suzumura, T. Araki, T. Natsumura, S. Masaki, M. Onozuka, H. Onabe, T. Yamamura and K. Yasuhira, in: *Proc. ECCM-8*, Vol. 4, I. C. Visconti (Ed.), pp. 57–64 (1998).
5. Y. Kogo, H. Hatta, H. Kawada, T. Shigemura, H. Onabe, T. Mizutani and F. Tomioka, *J. Compos. Mater.* **32** (11), 1016–1035 (1998).
6. Y. Sato and F. Nagai, *Bull. Jap. Soc. Mech. Engng.* **69** (575), 1617–1623 (1966) (in Japanese).
7. Y. Sato, *J. Jap. Soc., Mech. Engng.* **44** (386), 3371–3377 (1978) (in Japanese).
8. T. Hattori, K. Ikegami and H. Shiratori, *J. Japan Soc. Mech. Engng.* **A44**, 845–853 (1978) (in Japanese).
9. Y. Nose, K. Ikegami and H. Shiratori, *J. Japan Soc. Mech. Engng.* **A45**, 81–91 (1978) (in Japanese).
10. A. P. Coppa, in: *Proc. Japan–US CCM-III*, pp. 297–306 (1986).
11. K. Goto, H. Hatta, H. Takahashi and H. Kawada, *J. Am. Ceram. Soc.* **84** (6), 1327–1333 (2001).
12. Y. Kogo, H. Hatta, H. Kawada and T. Machida, *J. Compos. Mater*. **32** (13), 1273–1294 (1998).
13. For example, T. J. Mackin, T. E. Purcell, M. Y. He and A. G. Evans, *J. Am. Ceram. Soc.* **78** (7), 1719–1728 (1995).
14. T. Chang, T. Nakagawa and A. Okura, *Report of the Institute of Industrial Science*, The University of Tokyo **35**, 8 (1991).
15. For example, Y. Sato, Strength and plasticity of materials, in: *Atarashii Kikai Kogaku*, No. 4, p. 28. Morikita Shuppan Co. Ltd. (1980) (in Japanese).